Advances in Science and Technology Research Journal, 2026, 20(1), 501–509 https://doi.org/10.12913/22998624/211615 ISSN 2299-8624, License CC-BY 4.0

# The influence of abrasive material variations in sandblasting on surface roughness and corrosion rate of mild steel SS400

Akbar Zulkarnain<sup>1\*</sup>, Fyrdha Nur Sannya Hardyanti<sup>1</sup>, Henry Widya Prasetya<sup>1</sup>, Dadang Sanjaya Atmaja<sup>1</sup>, Dimas Adi Perwira<sup>1</sup>

- <sup>1</sup> Railway Mechanical Technology, Indonesian Railway Polytechnic, Tirta Raya Street, Madiun City, East Java, Indonesia
- \* Corresponding author's e-mail: akbar@ppi.ac.id

#### **ABSTRACT**

Corrosion is the degradation of metals due to electrochemical reactions with their environment, a critical issue affecting the longevity of mild steel train walls. In mild steel train walls, corrosion accelerates structural damage, necessitating effective surface treatment methods. Sandblasting, a key surface preparation technique, enhances adhesion and corrosion resistance by increasing surface roughness. This study investigates the impact of different abrasive materials silica sand, aluminum oxide, and steel grit on the surface roughness and corrosion rate of SS400 mild steel. Specimens ( $80 \times 80 \times 2$  mm) were prepared and treated via sandblasting, followed by surface roughness measurements and electrochemical corrosion testing. Results showed that steel grit produced the highest surface roughness ( $62.08 \mu m$ ), while silica sand yielded the lowest corrosion rate (0.0000175 mm/year). In contrast, despite its lower roughness, silica sand demonstrated superior corrosion inhibition compared to aluminum oxide and steel grit, suggesting that optimal abrasives for SS400 steel depend on balancing roughness and electrochemical performance. For applications prioritizing coating adhesion such as railway carbody repainting, steel grit is more suitable, whereas silica sand is preferable in scenarios where minimizing corrosion rate is the primary objective. These findings provide critical insights and practical guidance for selecting optimal abrasives in industrial sandblasting applications, particularly for the maintenance of train walls and similar large steel structures.

Keywords: abrasive blasting, corrosion rate, electrochemical test, railway transportation, surface modification.

## **INTRODUCTION**

Railway transportation has become increasingly vital in Indonesia's infrastructure development, with passenger demand growing due to its perceived safety and comfort. However, the structural integrity of train carbodies, predominantly manufactured from mild steel (SS400), faces significant challenges from corrosion. This degradation process, an electrochemical reaction between metal surfaces and environmental elements [1, 2], is particularly accelerated in tropical climates characterized by high humidity and frequent rainfall [3, 4]. The corrosion-induced deterioration of carbody components not only compromises passenger safety but also increases maintenance costs and reduces operational lifespan [5, 6].

Surface preparation through sandblasting has emerged as a critical pretreatment method in corrosion protection systems. This process employs abrasive materials such as silica sand, aluminum oxide (Al<sub>2</sub>O<sub>3</sub>), and steel grit to clean surfaces and create optimal roughness for coating adhesion [7, 8]. While conventional abrasives demonstrate varying degrees of effectiveness, significant limitations persist. Silica sand, despite its costeffectiveness, poses serious health hazards and inconsistent performance [9, 10]. Aluminum oxide offers moderate surface modification but may leave residual embedments [11, 12], while steel grit provides superior roughness but requires careful parameter control to prevent excessive surface damage [13, 14].

Received: 2025.08.31

Accepted: 2025.10.01

Published: 2025.11.21

Existing studies have predominantly focused on either surface roughness characteristics or corrosion resistance in isolation, with limited investigation into their combined effects on mild steel substrates. Furthermore, the specific performance of these abrasives under tropical environmental conditions remains poorly documented. Current literature lacks comprehensive comparisons of how different abrasive types influence both the immediate surface characteristics and long-term electrochemical behavior of SS400 steel, particularly in railway applications where cyclic wet-dry exposure is prevalent.

This study advances corrosion science by integrating surface profilometry and electrochemical testing into a unified framework, enabling a systematic correlation between abrasive-induced surface topography and corrosion resistance. Unlike previous works that addressed these parameters separately, this research provides a holistic assessment under simulated tropical conditions, thereby filling a critical gap in the literature. The novelty of the study lies in (1) establishing quantitative evidence of the relationship between surface roughness and corrosion resistance of SS400 mild steel, and (2) tailoring the evaluation to railway applications in tropical environments, where accelerated degradation mechanisms are most pronounced.

The investigation pursues three specific objectives: (1) to characterize the surface roughness profiles generated by different abrasive materials using optical profilometry, (2) to quantify the corrosion rates of treated surfaces through potentiodynamic polarization testing, (3) to determine the optimal abrasive type for maximizing both coating adhesion and corrosion protection in tropical railway applications. This structured approach ensures logical flow from problem identification through to solution development, while clearly positioning the study within the existing body of knowledge and highlighting its original contributions to the field.

#### **MATERIAL AND METHODS**

# Method of collecting data

Data were collected through two primary methods: experimental observation and literature review. Primary data were obtained from a series of tests conducted on SS400 steel plates, including specimen dimension measurements, standardized surface cleanliness assessments, electrochemical testing, and surface roughness measurements. Meanwhile, secondary data were compiled from various scientific reference sources such as journals, research reports, and technical publications to support the analysis. These secondary materials encompassed studies on types of abrasive materials, surface preparation methods, electrochemical testing techniques, roughness measurement standards, and the influence of abrasive materials on surface characteristics and corrosion rates.

In this study, three types of variables were established for testing purposes. The independent variable was defined as the type of abrasive material (steel grit, aluminum oxide, and silica sand) used in the sandblasting process. Control variables remained constant throughout the research, including the SS400 steel specimen material, plate dimensions, and the type of applied coating. The dependent variables consisted of two experimental outcome parameters: surface roughness levels and corrosion rate values derived from the experimental process. The establishment of these variables was implemented to ensure the reliability and validity of the research data.

#### Research tools and materials

The following tools and materials were utilized in this study (Table 1).

# **Specimen preparation**

The research specimens were fabricated from 2 mm-thick SS400 mild steel plates, cut into 24 specimens measuring 80 × 80 mm using an HGN 31/8 automatic cutting machine (Figure 1a). Each specimen was assigned a unique identification code based on the abrasive treatment type to be applied: Group A (A.1–A.8) for steel grit G25, Group B (B.1–B.8) for aluminum oxide G20, and Group C (C.1–C.8) for 20-mesh silica sand (Figure 1b). Prior to treatment, all specimens were cleaned with alcohol to remove surface contaminants.

# Sandblasting process

Surface preparation was conducted using the dry sandblasting method at a pressure of 8 bar with a nozzle distance of  $15 \pm 5$  cm from the specimen surface (Figure 2a). Three types of abrasive materials were applied separately to

Table 1. Tools, materials, and specifications

Name	Specifications	Application		
SS400 steel plate	Composition: Fe (98.3%), C (0.16%), Si (0.25%), Mn (1.45%), P (0.03%), S (0.02%)	Base material for test specimens		
Steel grit G25	Hardness: 50 HRC; density: 7.6 g/cm³	Abrasive material for Group A sandblasting		
Aluminum oxide G20	Hardness: 9 Mohs; composition: Al₂O₃ (≥95%)	Abrasive material for Group B sandblasting		
Silica sand	Hardness: 7 Mohs; particle shape: sub- angular	Abrasive material for Group C sandblasting		
Sandblasting machine	Operating pressure: 8 bar; sandpot capacity: 100 lbs	Surface preparation of specimens		
HGN 31/8 cutting machine	Capacity: 8×3100 mm; power: 11 kW	Cutting SS400 plates into 80×80×2 mm specimens		
Surface profile gauge	Range: 0–1000 μm; accuracy: 2 μm (Elcometer 123)	Measuring surface roughness post-sandblasting		
Corrtest potentiostat	Scan rate: 10 mV/s; electrode: SCE (reference)	Electrochemical corrosion rate testing		
Spraygun	-	Application of epoxy primer coating at a 1:3:1 ratio (primer:epoxy:thinner)		
3.5% HCl solution	Volume: 500 ml; concentration: 3.5%	Corrosive medium for electrochemical testing		
Graduated cylinder	-	Measuring volumes of coating solutions and electrolytes		



Figure 1. Cutting (a) and naming speciments (b)

each specimen group with a constant duration of 30 seconds per specimen. This process aimed to: (1) remove surface oxides and contaminants, (2) create a uniform roughness profile, and (3) enhance coating adhesion. Following sandblasting, abrasive residue was removed using compressed air prior to further testing (Figure 2b).

## Surface roughness testing

Surface roughness was evaluated using the arithmetic mean roughness parameter (Ra),

which represents the average deviation of surface peaks and valleys from the mean line. Surface roughness measurement was performed using an Elcometer 123 surface profile gauge in accordance with the ASME B46.1 standard. The instrument was calibrated beforehand using a glass substrate prior to measurement. For each specimen, three measurements were taken at distinct locations (center and two diagonal points) to obtain the average surface roughness value (Ra). The testing procedure included: (1) placement of the specimen on a flat surface, (2)



Figure 2. Sandblasting (a) and surface cleaning ceck (b)

activation of the instrument with needle contact against the surface, (3) recording of the value once the needle stabilized, and (4) post-measurement calibration verification.

#### Data analysis

Data analysis was conducted using SPSS software. Surface roughness data were statistically analyzed to compare the effects of each abrasive material. Corrosion rates were calculated using the Tafel method derived from polarization curves. The correlation between surface roughness and corrosion rates was evaluated for all three types of abrasive materials.

## **RESULT AND DISCUSSION**

## **Surface roughness**

The analysis revealed significant variations in surface roughness (Ra) across SS400 steel specimens treated with distinct abrasive materials, as shown in the graphical results (Figure 3).

The results demonstrate that abrasive material selection has a decisive influence on surface roughness development in SS400 mild steel. Steel grit generated the highest surface roughness (62.08  $\mu m$ ), nearly three times greater than silica sand (22.7  $\mu m$ ), with aluminum oxide producing an intermediate effect (41.79  $\mu m$ ). This outcome is consistent with the intrinsic hardness and angular morphology of the abrasive particles: steel grit, being dense and sharp-edged, induces deeper micro-valleys and higher peaks, while silica sand, with its lower hardness and rounded geometry,

results in less pronounced topographic features. These findings corroborate earlier reports that particle hardness and angularity strongly determine the intensity of surface modification during blasting processes [15,16].

Increased surface roughness is widely recognized as a prerequisite for enhancing coating adhesion and corrosion resistance. Okokpujie et al. demonstrated that corrosion protection performance significantly improves when roughness values exceed 30-40 µm, owing to mechanical interlocking and improved wettability between coating and substrate [17]. The present results show that steel grit, with Ra above 60 µm, surpasses this critical threshold, suggesting superior long-term protective performance. This observation aligns with recent work found that grit blasting not only improved microhardness but also markedly reduced corrosion current densities in Ni-W/SiC nanocomposite coatings [18,19]. Conversely, the relatively low roughness produced by silica sand may compromise coating adhesion and accelerate localized corrosion under aggressive tropical conditions.

Despite these advantages, the possibility of abrasive residue embedding remains a practical concern. Alumina or steel particle embedment can alter surface chemistry and create galvanic micro-cells, influencing corrosion kinetics [20,21]. While the results clearly identify steel grit as the most effective abrasive in terms of surface roughening, further investigation into potential contamination effects is warranted, particularly for tropical railway applications where cyclic wet dry exposure intensifies electrochemical degradation. Overall, these findings contribute novel insight by establishing a direct

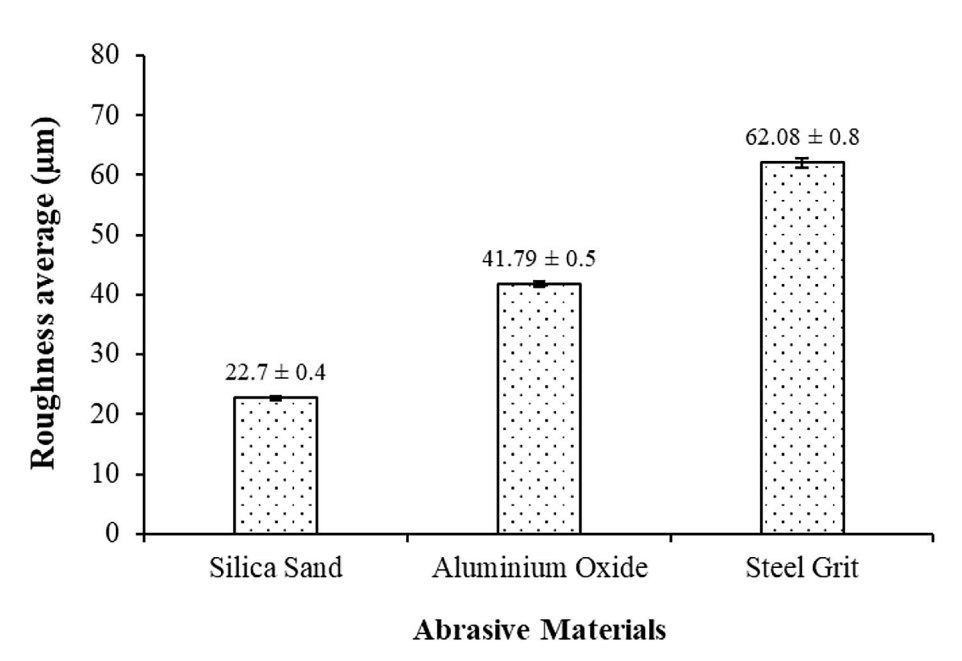


Figure 3. Surface rougness average

and quantifiable relationship between abrasive induced surface morphology and corrosion resistance, extending the applicability of surface engineering strategies to infrastructure maintenance in tropical environments.

#### **Corrosion rate**

Based on the corrosion rate test results using the electrochemical method, a normality test was conducted (Table 2).

Figure 4 depicts the corrosion rate of SS400 mild steel specimens treated with different abrasive materials. The corrosion rates are clearly differentiated: silica sand resulted in the highest rate at  $5.39 \pm 0.12 \times 10^{-4}$  mm/year, aluminum oxide significantly lowered it to  $1.45 \pm 0.14 \times 10^{-4}$  mm/year, and steel grit achieved the lowest rate of  $0.14 \pm 0.01 \times 10^{-4}$  mm/year. These findings highlight a

strong dependence of corrosion performance on the type of abrasive used during surface treatment, with steel grit markedly outperforming both silica sand and aluminum oxide in mitigating corrosion in the simulated tropical railway environment.

The observed gradient in corrosion rates highest with silica sand, intermediate with aluminum oxide, and lowest with steel grit aligns with established understanding of how surface roughness and morphology affect electrochemical behavior. Rougher surfaces can enhance coating adhesion and reduce dissolution; however, excessively rough or irregular profiles may trap corrosive agents and compromise protection. Notably, that abrasive blasting which increases surface roughness also significantly improves corrosion resistance in carbon steel substrates, corroborating our finding that steel grit, which produces the roughest surface, yields the lowest corrosion rates [22, 23].

Table 2. Normality test of corrosion rate

Tests of Normality							
Parameter	Kolmogorov-Smirnov <sup>a</sup>		Shapiro-Wilk				
	Statistic	df	Sig.	Statistic	df	Sig.	
Silica sand	0.274	6	0.178	0.853	6	0.166	
Aluminium oxide	0.309	6	0.075	0.851	6	0.159	
Steel grit	0.211	6	0.200*	0.865	6	0.208	

**Note**: \* This is a lower bound of the true significance, a – Lilliefors significance correction.

The normality test results for corrosion rates revealed that the Shapiro-Wilk significance values in the Sig. column exceeded 0.05. This indicates that the data followed a normal distribution. Following the normality test, the experimental results were obtained as shown in Figure 4.

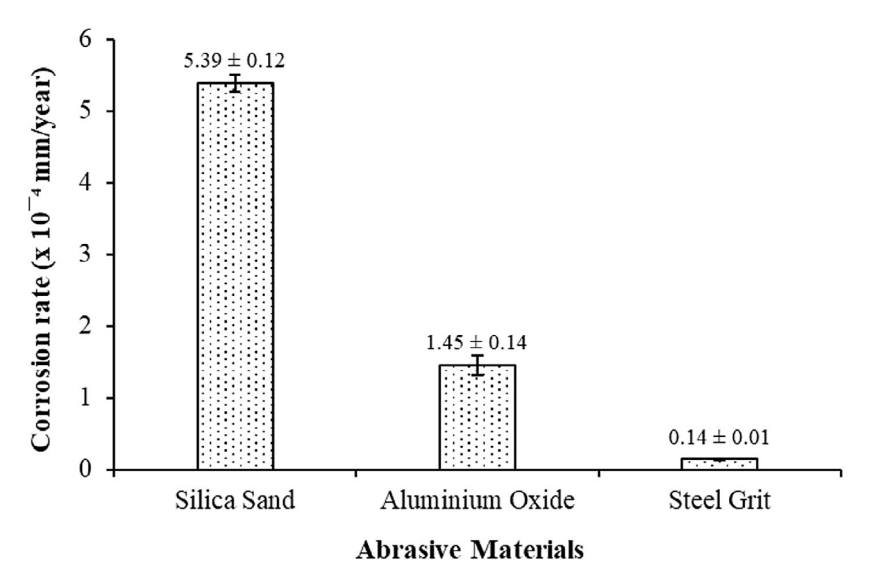


Figure 4. Corrosion rate

Moreover, Sandblasting with quartz or silica has sometimes shown detrimental effects on corrosion resistance. For instance, that S235JR steel sandblasted with quartz exhibited significantly increased roughness and reduced corrosion resistance compared to non-sandblasted specimens [24, 25]. This behavior mirrors our results, where silica sand treatment yielded the highest corrosion rate. On the contrary, aluminum oxide provided moderate control over surface roughness and delivered substantially better corrosion performance, though still inferior to steel grit.

These findings suggest that the superior performance of steel grit stems from its ability to generate a surface profile conducive to robust mechanical interlocking of protective coatings, while avoiding the excessive destabilization seen with silica sand. Nonetheless, potential embedding of abrasive residues, particularly from metallic grit, must be considered as it can act as localized corrosion initiators or disrupt passivation behavior [26, 27]. Future work should thus evaluate the long-term stability of grit-blasted surfaces and explore post-treatment cleaning or passivation strategies to mitigate any negative effects from embedded particles. The relationship between surface roughness and corrosion rate is illustrated in the following figure (Figure 5).

Figure 5 shows the correlation between average surface roughness (Ra) and corrosion rate of SS400 mild steel treated with different abrasive materials. The data reveal a strong negative linear relationship, expressed by the regression equation y = -6.8867x + 58.213 with a high coefficient of determination ( $R^2 = 0.9132$ ). This indicates that

approximately 91% of the variation in surface roughness can be explained by changes in corrosion rate. In other words, specimens with higher surface roughness consistently exhibited lower corrosion rates, whereas smoother surfaces correlated with accelerated degradation.

The strong inverse relationship between surface roughness and corrosion rate confirms the critical role of surface morphology in influencing electrochemical performance. Increased roughness enhances the mechanical interlocking of protective coatings and improves surface wettability, thereby reducing the likelihood of coating delamination and corrosion initiation. This phenomenon is consistent that corrosion protection improves significantly when roughness surpasses a critical threshold (30–40 µm), enabling coatings to anchor more effectively to the substrate [28, 29].

The present results further align that gritblasted steel surfaces with higher Ra values exhibited superior corrosion resistance compared to smoother substrates, due to increased microtopographic anchoring sites that restricted electrolyte penetration [30, 31]. Similarly, that rougher surfaces produced by steel grit blasting significantly outperformed quartz-sand-blasted specimens in terms of corrosion resistance, underlining the importance of abrasive type in achieving optimal surface profiles [32, 33].

However, while higher roughness generally improves adhesion, excessively rough or contaminated surfaces may trap corrosive residues or abrasive particles, potentially initiating localized corrosion. Embedded abrasive fragments can alter local electrochemical behavior, sometimes

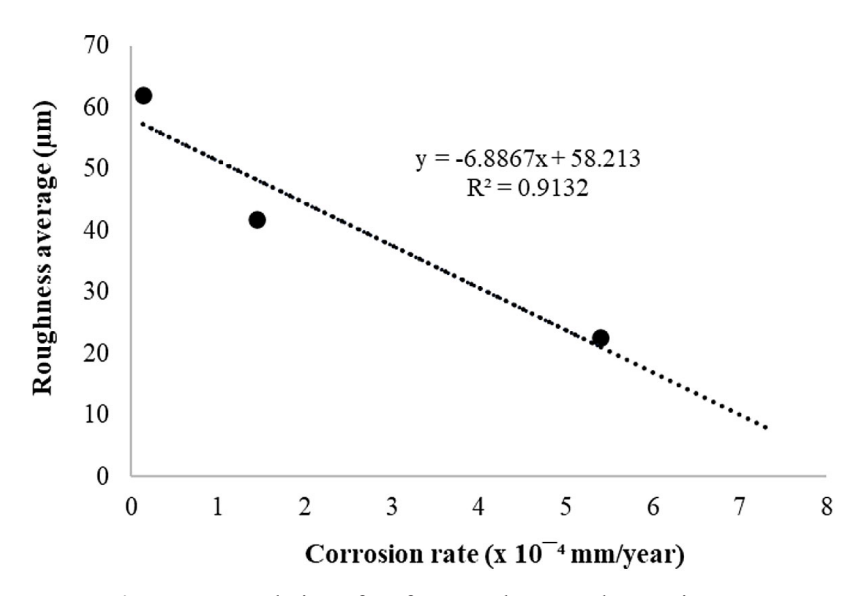


Figure 5. Correlation of surface roughness and corrosion rate

counteracting the protective benefits of increased roughness [34, 35]. Therefore, the nearly linear correlation observed here underscores the dominant effect of roughness in the current study, but also suggests that future work should investigate the long-term stability of these surfaces under tropical cyclic wet dry exposures.

#### **CONCLUSIONS**

Based on the research results and analysis, the following conclusions are drawn:

- 1. Surface roughness testing on SS400 carbody specimens revealed that steel grit produced the highest surface roughness (62.08 μm), followed by aluminum oxide (41.79 μm), with silica sand yielding the lowest value (22.7 μm).
- 2. Electrochemical corrosion rate testing demonstrated that steel grit exhibited the lowest corrosion rate ( $0.14 \pm 0.01 \times 10^{-4}$  mm/y), indicating superior corrosion resistance compared to aluminum oxide ( $1.45 \pm 0.14 \times 10^{-4}$  mm/y) and silica sand ( $5.39 \pm 0.12 \times 10^{-4}$  mm/y).
- 3. Steel grit is the most effective abrasive material for inhibiting corrosion in SS400 steel. Sandblasting with steel grit generated the highest surface roughness, resulting in superior coating adhesion and the lowest corrosion rate. In contrast, silica sand produced the weakest coating adhesion and highest corrosion rate.

Beyond these technical findings, this study contributes new scientific understanding by demonstrating a direct and quantifiable relationship between surface roughness and corrosion resistance under tropical exposure. The integration of profilometric and electrochemical methods within one framework represents a methodological advancement over earlier works that treated these aspects independently. The novelty of the study lies in bridging the gap between surface engineering and corrosion science, while providing evidence-based insights specific to tropical railway environments where cyclic wet dry conditions accelerate steel degradation. These outcomes not only enrich the fundamental literature on corrosion science but also deliver practical guidance for optimizing abrasive selection in railway maintenance, aligning with the broader goals of sustainable infrastructure management.

#### **REFERENCES**

- 1. Hirata Y., Fujii H., Sato C., Serizawa H. Welding and Joining. In: Innovative Structural Materials: Reducing Weight of Transportation Equipment. Singapore: Springer Nature Singapore; 2023:127–222. https://doi.org/10.1007/978-981-99-3522-2\_4
- Saji V.S. Corrosion and materials degradation in electrochemical energy storage and conversion devices. ChemElectroChem 2023;10(11):e202300136. https://doi.org/10.1002/celc.202300136
- 3. Daniel EF., Wang C., Li C., Dong J., Udoh II., Zhang D., Zhong S. Evolution of corrosion degradation in galvanised steel bolts exposed to a tropical marine environment. J. Mater. Res. Technol.

- 2023;27:5177–90. https://doi.org/10.1016/j.jmrt.2023.10.295
- Song D., Zhou Q., Xu D., Zheng Y., Cui Z., Wan H. Corrosion prediction and factors analysis of 2A12 aluminum alloy in marine environment based on data mining. Mater. Today Commun. 2025;42:111324. https://doi.org/10.1016/j.mtcomm.2024.111324
- Liu Q., Cao Y., Chen S., Xu X., Yao M., Fang J., Liu G. Hot-dip galvanizing process and the influence of metallic elements on composite coatings. J. Compos. Sci. 2024;8(5):160. https://doi.org/10.3390/jcs8050160
- 6. Li H., Yan H., Wang X., Li L. Corrosion fatigue evaluation of suspender cables in railway bridges considering the effect of train-induced flexural vibration. J. Bridge Eng. 2024;29(12):04024089. https://doi.org/10.1061/JBENF2.BEENG-6952
- Britton DA., Penney D., Malla AD., Mehraban S., Sullivan J., Goldsworthy M., Challinor C. Effect of antimony additions on the microstructure and performance of Zn–Mg–Al alloy coatings. npj Mater. Degrad. 2024;8(1):62. https://doi.org/10.1038/ s41529-024-00481-7
- Rudawska A. Mechanical surface treatment of adherends for adhesive bonding. Prog. Adhes. Adhes. 2023;7:113–69. https://doi. org/10.1002/9781394198375.ch3
- Anaç N., Doğan Z. Effect of organic powders on surface quality in abrasive blasting process. Processes 2023;11(7):1925. https://doi.org/10.3390/ pr11071925
- 10. Kumari R. Plasma-sprayed Al<sub>2</sub>O<sub>3</sub>-TiO<sub>2</sub>-YSZ composite coating on EN31 steel: microstructural and tribological properties for improved agricultural tool durability. J. Mater. Eng. Perform. 2025;1–12. https://doi.org/10.1007/s11665-025-11318-y
- 11. Du J., Huang Q., Liu P., Fu Y., Liu J., Chen X., Yuan Y. Review of recent advances in chemical sand production control: materials, methods, mechanisms, and future perspectives. Energy Fuels 2024;38(22):21845–72. https://doi.org/10.1021/acs.energyfuels.4c04114
- Rasheed T., Ferry DB., Iqbal ZF., Imran M., Usman M. Cutting-edge developments in MXene-derived functional hybrid nanostructures: a promising frontier for next-generation water purification membranes. Chemosphere 2024;141955. https://doi. org/10.1016/j.chemosphere.2024.141955
- 13. Zhao W., Liu D., Shi H., Hao Z., Zhao J. The effect of surface gradient nanostructure and compressive residual stress on fretting fatigue of A100 ultrahigh strength steel by ultrasonic surface rolling process. Int. J. Fatigue 2025;193:108775. https://doi.org/10.1016/j.ijfatigue.2024.108775

- 14. Gutema EM., Lemu HG. Conventional machining of metal matrix composites towards sustainable manufacturing present scenario and future prospects. J. Compos. Sci. 2024;8(9):356. https://doi.org/10.3390/jcs8090356
- 15. Oranli E., Ma C., Gungoren N., Astaraee AH., Bagherifard S., Guagliano M. Sand blasting for hydrophobic surface generation in polymers: experimental and machine learning approaches. Appl. Surf. Sci. Adv. 2024;23:100633. https://doi.org/10.1016/j.apsadv.2024.100633
- Wei F., Wei Y., Yao X., Li X., Wei Z., Zhang S., Zhu Q. Enhancing bond strength of heterogeneous metal-polymer components: the perspective of surface micro-nano morphology construction. J. Mater. Sci. 2025;1–36. https://doi.org/10.1007/s10853-025-10795-9
- 17. Okokpujie I.P., Tartibu L.K., Musa-Basheer H.O., Adeoye A.O.M. Effect of coatings on mechanical, corrosion and tribological properties of industrial materials: a comprehensive review. J. Bio-Tribo-Corros. 2024;10(1):2. https://doi.org/10.1007/ s40735-023-00805-1
- 18. Ma C., He H., Zhang H., Xia F., Li H. Impact of ultrasonic power density on the structure and performance of Ni-W-SiC composite nanocoatings. Surf. Coat. Technol. 2025;496:131641. https://doi. org/10.1016/j.surfcoat.2024.131641
- Huang P.C., Cheng C.H. Preparation and tribocorrosion behavior of electrodeposited Ni–W/SiC composite coatings. Wear 2024;558:205571. https://doi.org/10.1016/j.wear.2024.205571
- Katiyar P.K., Maurya R., Neetu. Corrosion behavior of ancient Indian iron artifacts: a comparative study. Metallogr. Microstruct. Anal. 2025;1–45. https://doi.org/10.1007/s13632-025-01240-z
- 21. Nazari H., Barati Darband G., Arefinia R. A review on electroless Ni–P nanocomposite coatings: effect of hard, soft, and synergistic nanoparticles. J. Mater. Sci. 2023;58(10):4292–4358. https://doi.org/10.1007/s10853-023-08281-1
- 22. Tawade P., Shembale S., Hussain S., Sabiruddin K. Effects of different grit blasting environments on the prepared steel surface. J. Therm. Spray Technol. 2023;32(5):1535–53. https://doi.org/10.1007/s11666-023-01585-3
- de Souza VP., da Silva Labiapari W., Lins VDFC. Stainless steels as a solution for corrosion and erosion problems involving grains in agribusiness sector applications. J. Mater. Res. Technol. 2024;30:5605–22. https://doi.org/10.1016/j.jmrt.2024.04.203
- 24. Bogatu N., Muresan AC., Mardare L., Ghisman V., Ravoiu A., Dima FM., Buruiana DL. The influence of different type materials of grit blasting on the corrosion resistance of \$235JR carbon steel. Inventions 2023;8(1):39. https://doi.org/10.3390/inventions8010039

- 25. Marquez-Herrera A., Saldaña-Robles A., Reveles-Arredondo JF., Dorantes-Flores JL., Gallardo-Hernandez EA., Capilla-González G. Effect of slide burnishing on the corrosion resistance and surface roughness on high strength steels. Adv. Mech. Eng. 2023;15(10):16878132231201794. https://doi.org/10.1177/16878132231201794
- 26. Friesen C.M., Pulfer J. Fluoropolymers in medical applications: recent progress and development. Chem. Rev. 2025. https://doi.org/10.1021/acs.chemrev.4c00996
- 27. Manu K.C., Madhushree C., Chandini M.S., Shree N., Hemanth S., Jeevan T.P. Corrosion in steel structures: a review. J. Mines Met. Fuels 2025;73(1). https://doi.org/10.18311/jmmf/2025/46985
- Wood R.J., Lu P. Coatings and surface modification of alloys for tribo-corrosion applications. Coatings 2024;14(1):99. https://doi.org/10.3390/coatings14010099
- 29. Ma Q., Yang Q., Zhang J., Ren F., Xia C., Chen F. Anti-corrosion properties of bio-inspired surfaces: a systematic review of recent research developments. Mater. Adv. 2024;5(7):2689–2718. https:// doi.org/10.1039/D3MA01058A
- 30. Cheng Z., Fu J., Kang P., Yao H., Mo F., Hu H. Surface topography optimization engineering: stabilizing zinc metal anode/aqueous electrolyte interfacial

- chemistry. Adv. Energy Mater. 2025;2405767. https://doi.org/10.1002/aenm.202405767
- 31. Ji W., Luo B., Wang Q., Yu G., Liu Z., Zhao Z., Liang J. Revealing the influence of surface microstructure on Li wettability and interfacial ionic transportation for garnet-type electrolytes. Adv. Energy Mater. 2023;13(21):2300165. https://doi.org/10.1002/aenm.202300165
- 32. Medvedovski E., Leal Mendoza G. Enamel (glassy) coatings for steel protection against high temperature corrosion. Adv. Appl. Ceram. 2023;122(3–4):145–69. https://doi.org/10.1080/17436753.2023.2231699
- 33. Dotta T.C., D'Ercole S., Iezzi G., Pedrazzi V., Galo R., Petrini M. The interaction between oral bacteria and 3D titanium porous surfaces produced by selective laser melting—a narrative review. Biomimetics 2024;9(8):461. https://doi.org/10.3390/biomimetics9080461
- 34. Reff C.M., Gamagedara K.U., Santefort D.R., Roy D. Tribo-electrochemical characterization of brush-scrubbed post-CMP cleaning: results for tartrate-supported removal of residual oxides from copper films. Lubricants 2025;13(7):301. https://doi.org/10.3390/lubricants13070301
- 35. Singh G., Singh R., Rao P.S. On modes of electrochemical machining: a comprehensive review. Adv. Mater. Process. Technol. 2024;1–39. https://doi.org/10.1080/2374068X.2024.2439703